Electronic structure, magnetism, and spin-dependent transport of $CeMnNi_4$

E. N. Voloshina,[1] Yu. S. Dedkov,[2*] M. Richter,[3] and P. Zahn[4†]

[1] *Max-Planck-Institut für Physik komplexer Systeme, Nöthnitzer Str. 38, 01187 Dresden, Germany*

[2] *Institut für Festkörperphysik, Technische Universität Dresden, 01062 Dresden, Germany*

[3] *IFW Dresden e.V., P.O. Box 270 116, 01171 Dresden, Germany*

[4] *Fachbereich Physik, Martin-Luther-Universität Halle-Wittenberg, 06099 Halle/Saale, Germany*

(Dated: November 25, 2005)

Abstract

Theoretical investigations of the electronic band structure and ferromagnetism of $CeMnNi_4$ have been performed by means of an LSDA approach. The calculated magnetic moment of $4.88\,\mu_B$ per formula unit is in good agreement with the value determined experimentally. Recent point contact Andreev reflection experiments show that this compound has a relatively large transport spin polarization. The calculations reveal a much smaller polarization of the density of states and transport coefficients at the Fermi level. A small shift of the Fermi level by about 0.1 eV raises the polarization values close to the experimental ones.

PACS numbers: 71.20.-b, 71.18.+y, 72.25.-b, 75.50.Cc

* e-mail: dedkov@physik.phy.tu-dresden.de

† also at Institut für Theoretische Physik, Technische Universität Dresden, 01062 Dresden, Germany

Controlling the spin of electrons within a device can produce surprising and substantial changes in its properties. A new generation of devices based upon manipulation of spins in solids may have entirely new functionality that could provide a foundation for totally new computational paradigms. Crucial to all spintronic devices are materials with a high spin polarization at the Fermi level, E_F. Ordinary metals, such as copper, have zero spin polarization, whereas ferromagnetic metals, such as iron, have spin polarization of about 40% or less at E_F. The ultimate spin-polarized materials attainable are the so-called half-metallic ferromagnets (HMF) which have the extreme limit of spin asymmetry [1]. In these materials the band structure splitting is such that only one spin channel has available states at the Fermi surface and hence all current must be carried by electrons with parallel spin. By definition, such materials are 100% spin-polarized. Practical examples include chromium dioxide (CrO_2) [2, 3], lanthanum strontium manganite ($La_{0.7}Sr_{0.3}MnO_3$) [4, 5], and some Heusler alloys [6]. In reality, obtaining half-metallic spin-electronic behavior is fraught with problems mainly due to the interfaces. Conversely, some materials whose bulk electrical conduction deploys both spin channels may, due to hybridization, form half-metallic interfaces with other materials. Besides the spin-polarization of the ferromagnetic material there are other factors which are crucial for the aim of spin injection. Among them the more important are: (i) Fermi velocity mismatch between the source of spin-polarized electrons and the collector, (ii) difficulties in thin film preparation, (iii) imperfections on the surface and in the bulk of HMF material.

Recently, some intriguing properties of $CeMnNi_4$, a ferromagnetic material with a high total magnetic moment of $4.95\,\mu_B$/f.u., were discovered [7]. As it was experimentally found this material has a relatively large Curie temperature of $T_C \sim 150\,\mathrm{K}$ and exhibits a large transport degree of spin polarization (DSP) [8] of about 66% determined by the point-contact

Andreev reflection (PCAR) method [9–11]. This fact allows one to speculate (or suggest) that this material is a HMF or close to this state.

In the present work we performed LSDA calculations of electronic band structure and magnetic properties of $CeMnNi_4$. Assuming a collinear ferromagnetic ground state, the magnetic moment was determined to be about $4.88\,\mu_B$/f.u. and mainly carried by Mn $3d$ states. In contradiction to the experimental result and suggestion that this material is HMF or close to this state, we found a rather low spin polarization at E_F of about (-20%). The ordinary and transport spin-polarization of $CeMnNi_4$ is subsequently discussed.

To obtain accurate total energies and detailed spin-resolved electronic structure information, the full-potential local orbital (FPLO) calculation scheme was applied [12]. In the scalar-relativistic calculations the local spin density approximation (LSDA) exchange and correlation potential of Perdew and Wang [13] was used. As the basis set, Ce $(4f, 5s, 5p, 5d, 6s, 6p)$, Mn $(3s, 3p, 3d, 4s, 4p)$, and Ni $(3s, 3p, 3d, 4s, 4p)$ states were employed. The lower-lying states were treated fully relativistically as core states. The treatment of the Ce $5s, 5p$, Ni $3s, 3p$, and Mn $3s, 3p$ semicore-like states as valence states was necessary to account for non-negligible core-core overlaps. The spatial extension of the basis orbitals was optimized to minimize the total energy. A $\mathbf{k}$-mesh of 735 points in the irreducible part of the Brillouin zone (13824 in the full zone) was used to ensure accurate density of states and band structure information, especially in the region close to the Fermi level.

Hexagonal $CeNi_5$ (Space group: $P6/mmm$) [Fig. 1(a)] may be considered as a parent compound for $CeMnNi_4$ (Space group: $F\bar{4}3m$) [Fig. 1(b)]. The latter crystallizes in the face-centered cubic $AuBe_5$ structure with lattice constant $a = 6.957\,$Å and with the following Wyckoff positions: Ce (0,0,0), Mn (1/4,1/4,1/4), and Ni (5/8,5/8,5/8) [14]. In order to determine the equilibrium lattice constant a fourth-order polynomial fit of the calculated

total energy vs. lattice constant dependence was performed. The LSDA lattice constant of 6.817 Å is by 2.5% smaller than the experimental one of 6.987 Å [7]. Note that the latter value is about 0.5% larger than the earlier tabulated experimental value [14]; this disagreement could point to difficulties in sample preparation.

In experimental work [7] the magnetization versus temperature, $M(T)$, for the $CeMnNi_4$ sample was obtained and it reveals a sharp ferromagnetic transition with $T_C \sim 150\,\mathrm{K}$. The signature of the ferromagnetic transition was also seen as a pronounced knee in the resistivity vs. temperature, $\rho(T)$, at the same temperature. From magnetization vs. field, $M(H)$, scan recorded at 5 K a saturation magnetization of $4.95\,\mu_B$/f.u. was obtained. While, in principle, in this compound all constituents (Ce, Ni, and Mn) may possess magnetic moments, the parent compound $CeNi_5$ is a Pauli paramagnet [15]. Therefore, one can assume that the ferromagnetic transition arises due to the ordering of the Mn moments. To verify this assumption we have calculated the total magnetic moment in dependence on the lattice constant together with the site-projected moments (Fig. 2). The calculated total magnetic moment of $4.88\,\mu_B$/f.u. at $a = 6.817\,\text{Å}$ is in good agreement with the experimental value. The theoretical value of the Mn magnetic moment is determined to be $3.92\,\mu_B$/f.u. and $4.04\,\mu_B$/f.u. for theoretical and experimental values of lattice constant, respectively. The rest magnetic moment is mainly due to the four Ni atoms, which together give $1.1\,\mu_B$/f.u., supplemented by a small contribution of antiferromagnetically polarized Ce ($-0.14\,\mu_B$/f.u.).

Since hexagonal $CeNi_5$ can be considered as a parent compound for $CeMnNi_4$ we calculate the total and partial densities of states (DOS and PDOS, respectively) for Ce and Ni in the former compound. The results shown in Fig. 3 are in agreement with previous calculations [15]. As it was shown the Stoner criterion for an instability toward ferromagnetism in this compound is not fulfilled, in agreement with the fact that no magnetic ordering has

been observed ($IN \approx 0.75 < 1$, where I is the Stoner integral and N is the DOS per spin at the Fermi energy).

Fig. 4 and Fig. 5 show total and partial DOS and spin-resolved electronic band structure of $CeMnNi_4$ at the LSDA lattice constant, respectively. The Ce $4f$ states are situated approximately 1 eV above Fermi level and they are weakly polarized. Ni (mostly $3d$) states are also weakly polarized, but in the opposite way. Mn (mainly $3d$) occupied sates are found in the region between 0.5 and 3.5 eV below E_F. It is remarkable that the Mn-$3d$ band width in the majority spin channel is much larger (about 3 eV) than in the minority one (about 1.5 eV). This disparity arises from different interaction partners available in the two spin channels. Majority spin Mn-$3d$ states are hybridized with the almost fully occupied Ni-$3d$ states that form a band of about the same width as in elemental Ni metal, due to the large Ni concentration. On the other hand, the minority spin Mn-$3d$ states are split off due to exchange interaction by more than 3 eV. Thus, they hybridize with the Ce-$4f$ states that are available at this energy, around 1 eV above Fermi level, and form a narrow band due to the small number of neighbors at slightly larger inter-atomic distance (4 Mn-Ce neighbors at 3.01 Å compared with 12 Mn-Ni neighbors at 2.88 Å). The described band structure explains the position of Fermi level in a valley of the DOS: the Ni-$3d$ band is virtually filled and the Mn-$3d$ band is split into a filled spin-up band and an empty spin-down band. What remains at Fermi level are broad *sp* (and Ce-$5d$) - bands.

The corresponding densities of states at E_F for spin-up and spin-down channels in $CeMnNi_4$ are $N_\uparrow = 0.96\,\mathrm{eV}^{-1}\cdot\mathrm{f.u.}^{-1}$ and $N_\downarrow = 1.54\,\mathrm{eV}^{-1}\cdot\mathrm{f.u.}^{-1}$ giving an electronic specific heat coefficient γ of $5.8\,\mathrm{mJ\,mol}^{-1}\cdot\mathrm{K}^{-2}$. Though the Fermi level is situated in a DOS valley, the DOS at E_F is comparable to values found in normal metals like Al (about $0.3\,\mathrm{eV}^{-1}\cdot\mathrm{atom}^{-1}$), and to the value found, e.g., in HMF CrO_2 ($N_\uparrow \approx 1.9\,\mathrm{eV}^{-1}\cdot\mathrm{f.u.}^{-1}$) [16].

The calculated spin polarization of the DOS at E_F, $P(N) = (N^{\uparrow} - N^{\downarrow})/(N^{\uparrow} + N^{\downarrow})$, of $CeMnNi_4$ amounts to -16% and -21% in case of experimentally determined and LSDA lattice constants, respectively. These values are substantially lower than the experimentally determined polarization of 66% [7]. This discrepancy may originate from two sources. That we will discuss subsequently: (i) off-stoichiometry of the sample and/or (ii) oversimplified analysis of the experimental data.

As it was previously pointed out by Mazin [8] the DSP for Andreev reflection can be interpreted in terms of spin dependent transport coefficients $(Nv)^{\uparrow,\downarrow}$ and $(Nv^2)^{\uparrow,\downarrow}$ for the limits of ballistic and diffusive transport, respectively, neglecting the state-dependent transmittance of the barrier between normal metal and superconductor. They correspond to the Sharvin conductance and the plasma frequency squared, respectively, and are given by Fermi surface integrals over Fermi velocities $v_{\mathbf{k}}$: $(Nv)^{\uparrow,\downarrow} \propto \int d^3\mathbf{k}\delta(E_{\mathbf{k}}^{\uparrow,\downarrow} - E_F)v_{\mathbf{k}}^{\uparrow,\downarrow}$ and $(Nv^2)^{\uparrow,\downarrow} \propto \int d^3\mathbf{k}\delta(E_{\mathbf{k}}^{\uparrow,\downarrow} - E_F)\left(v_{\mathbf{k}}^{\uparrow,\downarrow}\right)^2$. The behavior of the spin dependent quantities N, (Nv), and (Nv^2) is given for the theoretical lattice constant in Fig. 6 (upper panel) for energies around the Fermi level. At the Fermi level the obtained polarizations [Fig. 6 (lower panel)] are substantially smaller than in experiment, but for slight changes of the Fermi level (by approximately 0.1 eV), values close to the experimentally ones are reached. The effect is most pronounced for N, and is weaker for (Nv) and (Nv^2) because the spin asymmetry of the Fermi velocity is opposite to the spin asymmetry of the DOS. Possible discrepancies of the polarizations derived from PCAR measurements using a Blonder-Tinkham-Klapwijk (BTK) scheme [17] and derived from bulk electronic structure are elucidated by Xia *et al.* [18]. The BTK approach uses very simplified model barriers and parabolic electronic bands. In real tunneling experiments a large part of the current is carried by few electronic states of high transmission (compare Fig.1(d) in Ref. [18]). From the spin dependent Fermi

velocities shown in Fig. 7 it is evident that this selection may change the apparent spin polarization of the ferromagnet drastically. The highly conducting majority states (left panel: states on the tubes along Γ-L direction and close to Γ point) may cause an opposite spin polarization of current than the polarization of the DOS. So, the interpretation of Andreev reflection measurements in terms of bulk polarizations can be highly misleading. Another reason for the discrepancy of experimental results and theoretical values at the Fermi level could be given by stoichiometric variations of the sample. A slight change of the Fermi level's position (of about 0.1 eV) can lead to a drastic change of the DOS spin polarization up to approximately −70%. Such a shift would occur, e.g., if 5% of Mn is replaced by Ni during the preparation process. This knowledge can be used in future sample optimization to increase spin-polarization by controlled alloying of $CeMnNi_4$.

In conclusion, the spin-resolved electronic band structure, magnetic properties, and transport coefficients of $CeMnNi_4$, a recently investigated soft magnetic material with high transport spin polarization and high magnetic moment, were studied. The theoretically calculated value of magnetic moment is in good agreement with experiment. In difference to the high transport spin polarization derived from point-contact Andreev reflection, the calculated values for the bulk material are low. We suggest two possible reasons for this discrepancy: (i) oversimplified analysis of the experimental data in terms of model barriers and parabolic bands and (ii) possible small off-stoichiometry of the sample shifting the position of the Fermi level. We propose to study the influence of well-controlled off-stoichiometry on the transport spin polarization of $CeMnNi_4$.

This work has been supported by the DFG through SFB 463.

---

[1] W. E. Pickett and J. S. Moodera, Physics Today **54**, 39 (2001).

[2] K.-H. Schwarz, J. Phys. F: Met. Phys. **16**, L211 (1986).

[3] M. A. Korotin, V. I. Anisimov, D. I. Khomskii, and G. A. Sawatzky, Phys. Rev. Lett. **80**, 4305 (1998).

[4] W. E. Pickett and D. J. Singh, Phys. Rev. B **53**, 1146 (1996).

[5] P. K. de Boer, H. van Lenken, R. A. de Groot, T. Rojo, and G. E. Barberis, Solid State Commun. **102**, 621 (1997).

[6] R. de Groot, F. Mueller, P. van Engen, and K. Buschow, Phys. Rev. Lett. **150**, 2024 (1983).

[7] S. Singh, G. Sheet, P. Raychaudhuri, and S. K. Dhar, cond-mat/0509101 (2005).

[8] I. Mazin, Phys. Rev. Lett. **83**, 1427 (1999).

[9] A. F. Andreev, Zh. Eksp. Teor. Fiz. **46**, 1823 (1964).

[10] J. R. J. Soulen, J. M. Byers, M. S. Osofsky, B. Nadgorny, T. Ambrose, S. F. Cheng, P. R. Broussard, C. T. Tanaka, J. Nowak, J. S. Moodera, et al., Science **282**, 85 (1998).

[11] S. K. Upadhyay, A. Palanisami, R. N. Louie, and R. A. Buhrman, Phys. Rev. Lett. **81**, 3247 (1998).

[12] FPLO-5.00-18 [improved version of the original FPLO code by K. Koepernik and H. Eschrig, Phys. Rev. B **59**, 1743 (1999)]; http://www.FPLO.de (2005).

[13] J. P. Perdew and Y. Wang, Phys. Rev. B **45**, 13244 (1992).

[14] P. Villars and L. D. Calvert, *Pearson's Handbook of Crystallographic Data for Intermetallic Phases, vol.1-3* (American Society for Metals, Oh 44073, 1989).

[15] L. Nordström, M. S. S. Brooks, and B. Johansson, Phys. Rev. B **46**, 3458 (1992).

[16] I. Mazin, D. J. Singh, and C. Ambrosch-Draxl, Phys. Rev. B **59**, 411 (1999).

[17] G. E. Blonder, M. Tinkham, and T. M. Klapwijk, Phys. Rev. B **25**, 4515 (1982).

[18] K. Xia, P. J. Kelly, G. E. W. Bauer, and I. Turek, Phys. Rev. Lett. **89**, 166603 (2002).

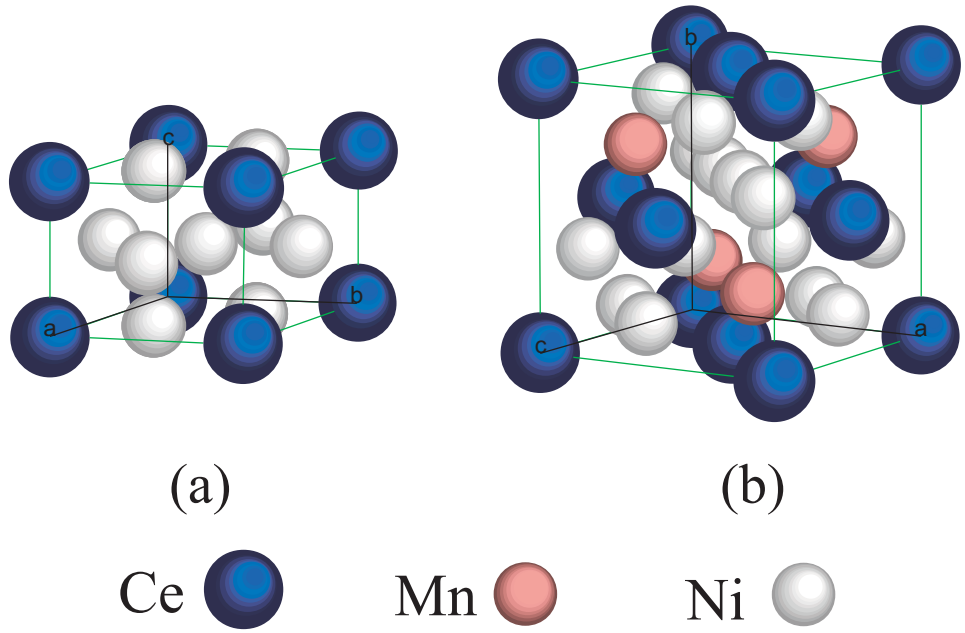

FIG. 1: (Color online) Crystallographic structures of (a) the hexagonal $CeNi_5$ and (b) the cubic $CeMnNi_4$ compound.

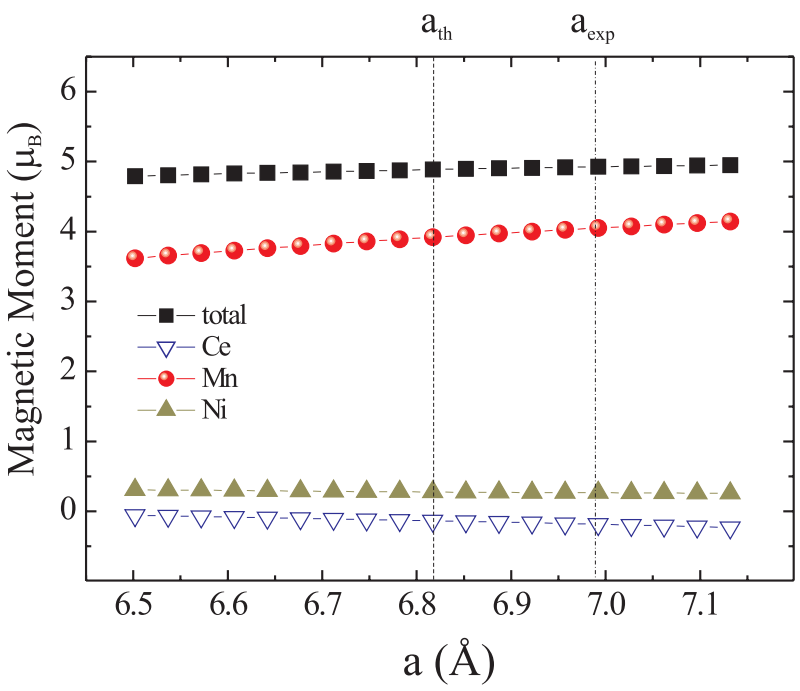

FIG. 2: (Color online) Total magnetic moment (black squares) as well as magnetic moments of Ce (open down-triangles), Mn (solid circles), and Ni (solid up-triangles) as a function of lattice constant of $CeMnNi_4$. The vertical lines mark theoretical and experimental values of the lattice constant, respectively.

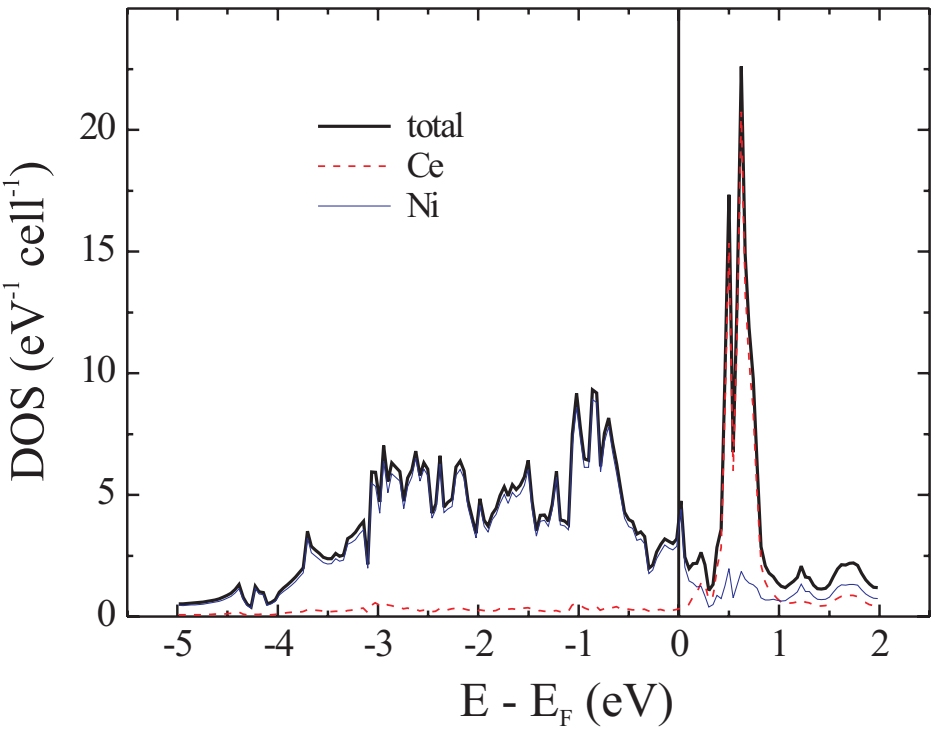

FIG. 3: (Color online) Total and partial density of states of the non-magnetic hexagonal $CeNi_5$.

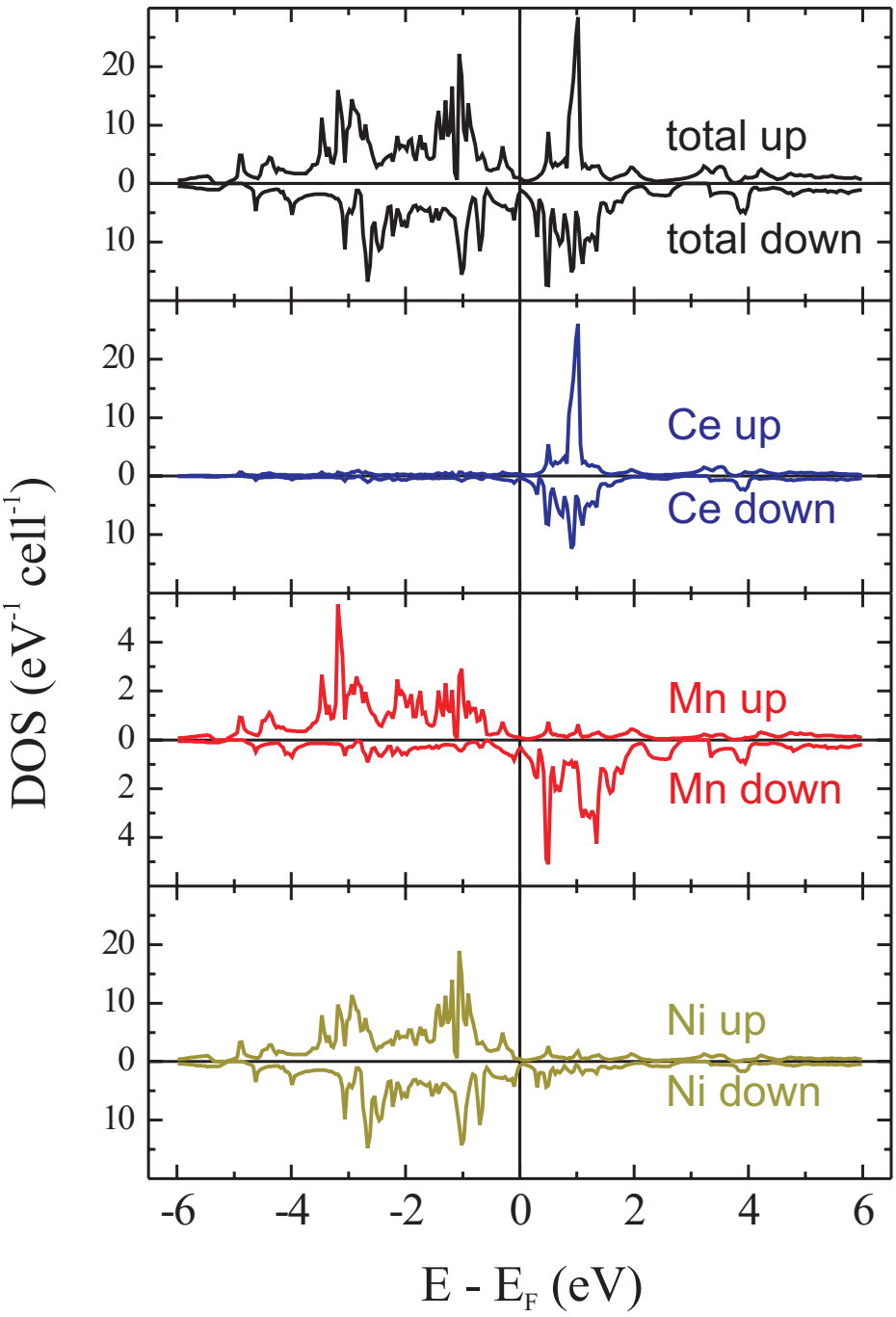

FIG. 4: (Color online) Total spin dependent DOS of $CeMnNi_4$ and the local DOS for Ce, Mn, and Ni (from top to bottom), respectively.

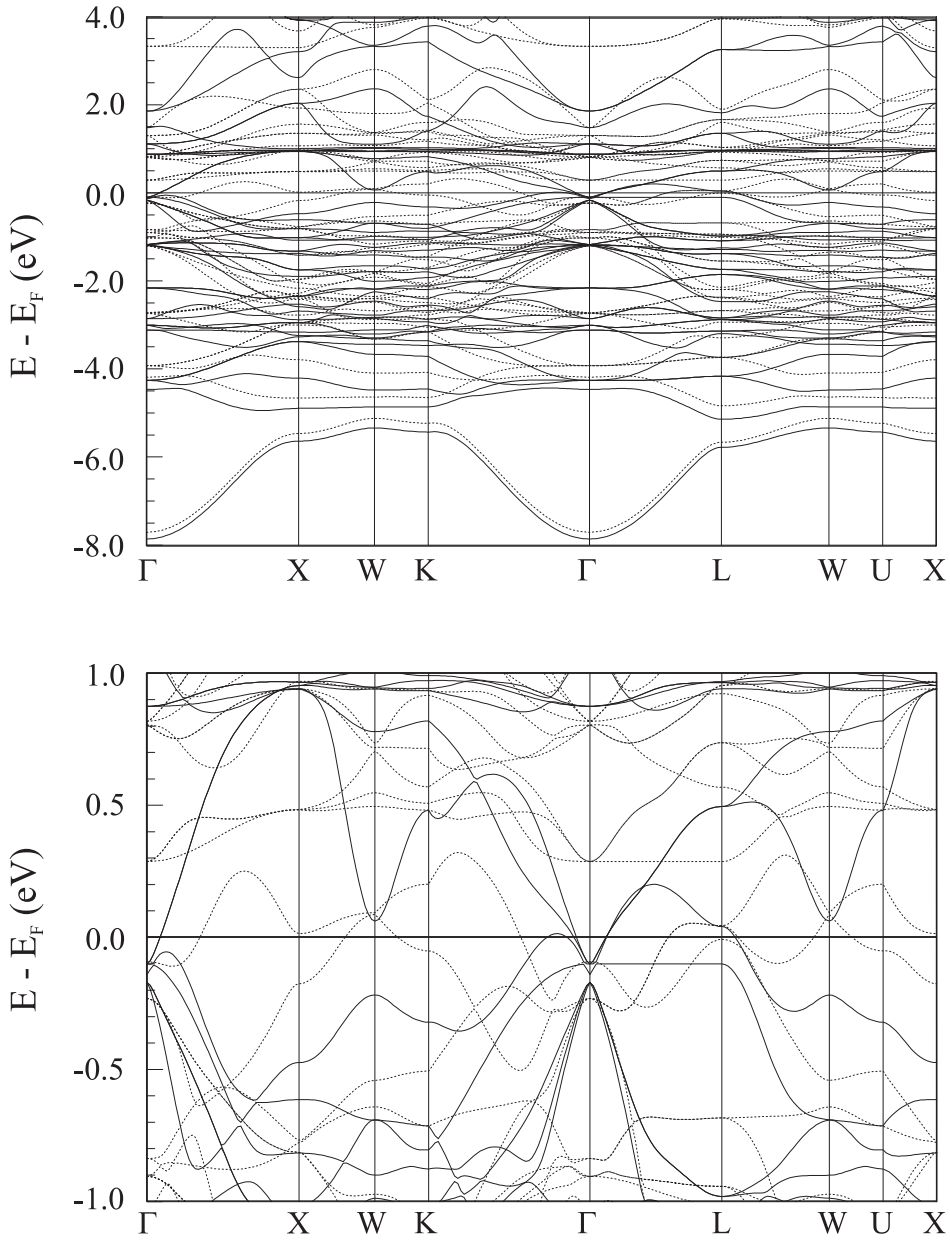

FIG. 5: The spin-resolved band structure of $CeMnNi_4$ over wide energy range (upper panel) and in the vicinity of Fermi level (lower panel). Solid and broken lines represent spin-up and spin-down electronic channels, respectively.

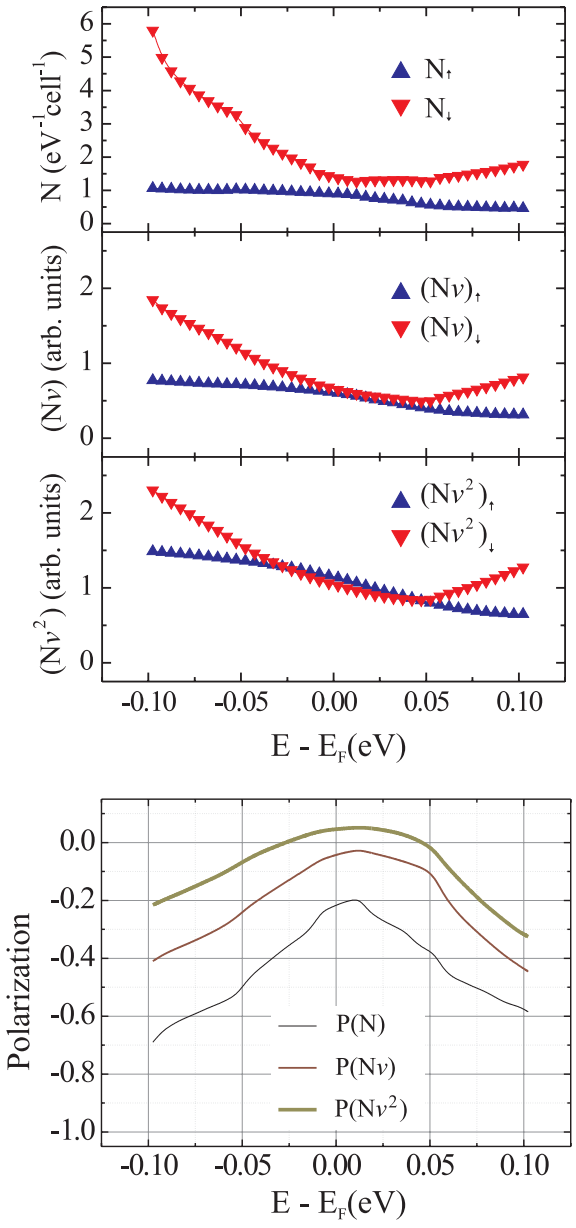

FIG. 6: (Color online) Spin dependent densities of states N, Sharvin conductance (Nv), plasma frequencies (Nv^2) (upper panel), and the derived spin polarizations for the theoretical lattice constant of $CeMnNi_4$ (lower panel).

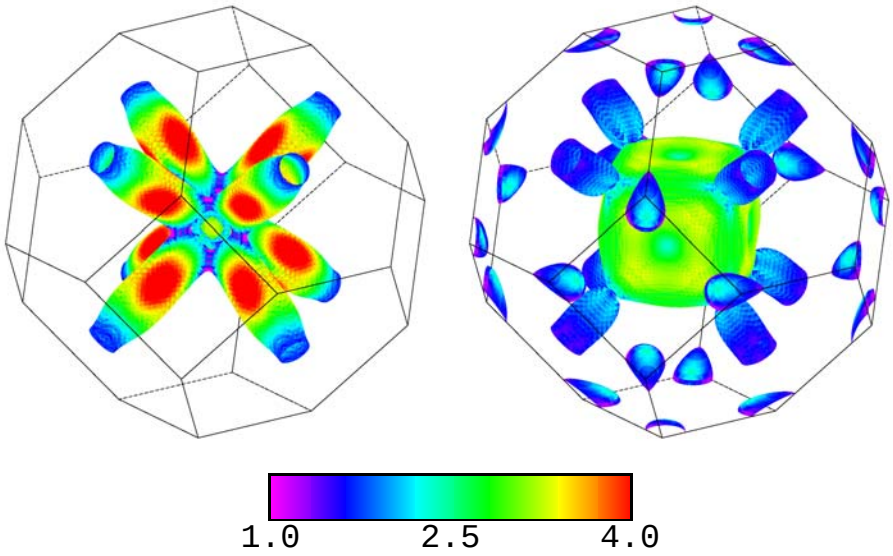

FIG. 7: (Color online) Fermi velocity distribution $|v_{\mathbf{k}}|$ for majority (left) and minority (right) spin states of $CeMnNi_4$ at the theoretical lattice constant (in units of 8.1×10^6 cm sec^{-1}).